# EXPERIMENTAL METHODS FOR EDDY CURRENT PROBE DESIGN AND TESTING

B. A. Auld and F. G. Muennemann

Edward L. Ginzton Laboratory
Stanford University
Stanford, CA 94305

G. L. Burkhardt

Southwest Research Institute
San Antonio, Texas

## INTRODUCTION

The purpose of this paper is to briefly review the influence of EC probe parameters on the performance of the complete NDE system and to describe experimental methods for measuring these parameters. Combined theory and experiment is required to quantify probe response, to design optimum probes for specific applications, to verify the reproducibility of probe performance during manufacture, and to verify the stability and precision of probe calibration. For these purposes it is necessary to consider, at least, the following probe parameters: (1) input impedance, for design of adjacent circuitry; (2) self-resonant frequency, for upper frequency limits of operation; (3) the ratio of probe field intensity to input current, for sensitivity; and (4) the distribution (or shape) of the flaw interrogating field generated by the probe — for control of flaw response, liftoff response and spatial resolution (i.e., separation of closely spaced flaws and discrimination against edges and corners).

Measurements of probe impedance and self-resonant frequency are standard, and will not be discussed here. For items (3) and (4) there are, in general, two classes of experiment that may be used: direct methods, where one measures probe characteristics with instruments which are independent of the probe (such as measuring the magnetic field distribution of a probe with a small Hall-effect probe), and perturbation methods, where one examines the field

distribution by observing changes in probe impedance due to a small perturbing object (i.e., a small magnetic sphere or a small hole in a metal sheet) as it is moved around in the field.

## THEORY OF EC PROBE OPERATION

During recent years a substantial amount of new theory has been generated for the flaw and liftoff responses of an EC prcbe. A brief review of this material, together with some of this year's extensions, is given by a companion paper (Muennemann, et al., 1984). At this point it is sufficient to recall that the general form of the general eddy current equation is

$$\Delta Z = \int_{\substack{\text{Flaw or} \\ \text{Workpiece}}} [H^2_{tan}(X,Y,\sigma,\omega)/I^2] \left\{ \begin{matrix} \text{Characteristic} \\ \text{Function} \end{matrix} \right\} dS \quad , \quad (1)$$

regardless of the probe geometry. This is an expression for the impedance change of the probe due to the presence of some "flaw," taken in the general sense to be a crack or inclusion, liftoff or tilt (the latter two effects being modeled as the removal of a parallel or tilted slice from the surface of the workpiece). It is seen that the integral, taken over a surface enclosing the "flaw" contains two factors. The first, enclosed in square brackets, is the square of the tangential magnetic field on the workpiece surface (the XY plane) normalized to the probe driving current. This factor, which is determined entirely by the probe itself, is controlled by the probe geometry, the conductivity of the workpiece $\sigma$ , and the operating frequency $\omega$ . The second factor, to be discussed in more detail in the companion paper, is a characteristic function of the "flaw" geometry, the conductivity of the workpiece $\sigma$ , and the operating frequency $\omega$ . It is seen from this that the "flaw" characteristics are viewed by the probe through a "window" or filter (i.e., the square bracket factor in the above integral). Probe response is strongly influenced by the nature of this filtering, so that probe geometry (as well as the operating frequency) are highly important in probe design. Furthermore, accurate inversion of the probe signal to determine the characteristic function of the flaw requires precise knowledge of the probe field strength and distribution. Since liftoff signals are in practice much larger than signals from cracks and inclusions it is important to design into the system some effective discrimination against these large unwanted signals. This is frequencly achieved by means of phase discrimination. Figure 1 shows, in the probe impedance plane, typical liftoff (dashed line) and flaw (solid line) signal trajectories generated by scanning over a flawed workpiece. It is seen that these lie at different (phase) orientations in the impedance

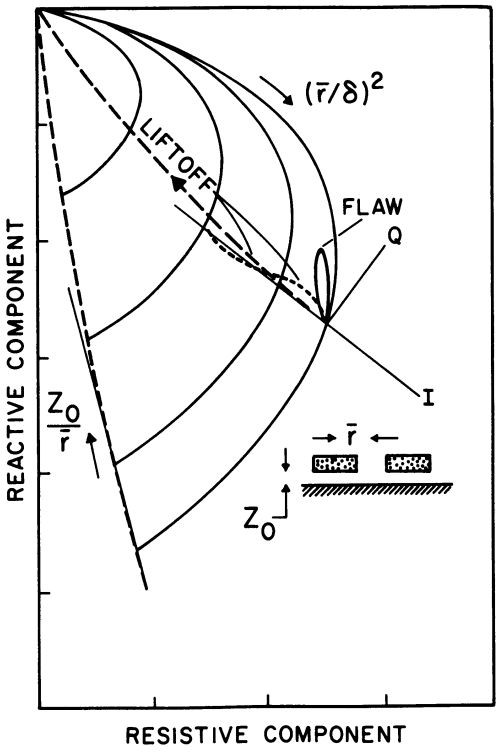


Fig. 1. Impedance plane traces of flaw and liftoff signals.

plane. Liftoff is minimized by reading the signals only along the axis marked Q in the figure (i.e., normal to the principal liftoff axis, marked I ). Standard EC test instrumentation is designed to permit this selection.

## INFLUENCE OF PROBE GEOMETRY ON FLAW AND LIFTOFF SIGNALS

Figure 2 shows three of the sample probe geometries investigated under this program. As was noted above, the effect of probe geometry on flaw and liftoff responses is determined by the probe field strength and shape in the first factor of Eq. (1). This factor influences flaw response and liftoff response in different ways because of differences in the characteristic functions for these two cases. Probe optimization for sensitivity requires a design that maximizes the Q-channel response of the first and minimizes that of the second. A simple example of the effect of coil configuration on flaw response is a comparison of a probe with the coil axes normal to the workpiece surface and another with the axes parallel to the surface. In the first arrangement the eddy currents form concentric circles about the coil axis and the field interrogating

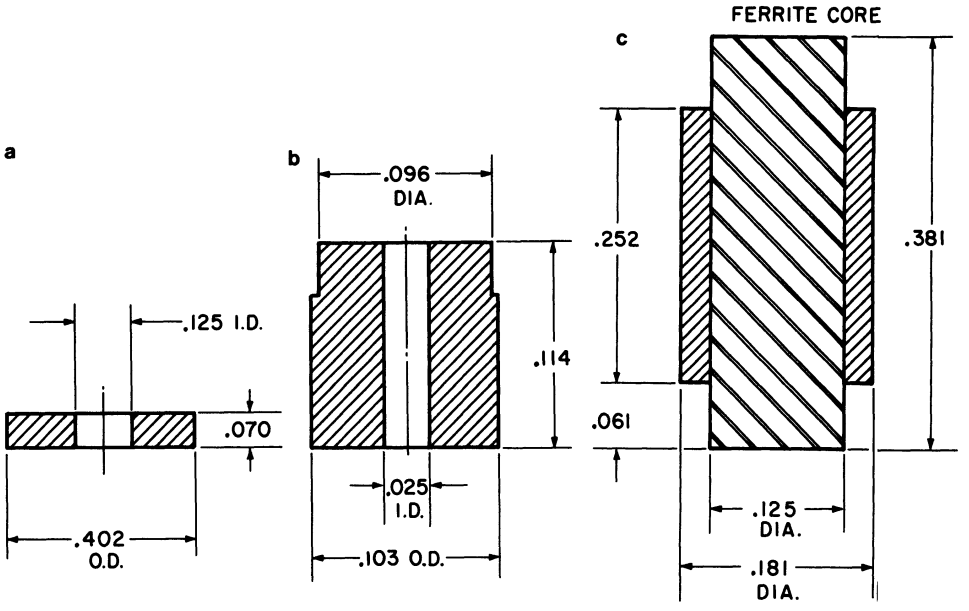


Fig. 2. Sample probe geometries. (a) Probe 3, 10 kHz air core, 500 turns; (b) probe 4, 200 kHz air core, 235 turns; (c) probe 2, 10 kHz ferrite core, 400 turns.

a flaw is highly nonuniform. The second arrangement has a region of essentially uniform field directly under the probe. These differences profoundly affect the flaw signal, with somewhat stronger signals predicted for the second (or horizontally-oriented) geometry. Flaw signals are also affected by the proportions of a coil (Fig. 2), regardless of its orientation, as are the liftoff signals. Figure 3 shows theoretically predicted liftoff signals for the two air core coils in Fig. 2, where the amplitude and phase variables are in the notation of Bahr and Cooley (1983). These are universal curves for arbitrary frequency and workpiece conductivity, the two variables entering into the definition of skin depth $\delta$. In the same figure is shown the Q-channel liftoff, measured on a ferrite core probe over a Ti 6-4 workpiece. This is observed to have a very different behavior moving toward small $\delta$ than does the I-channel liftoff. A similar effect is predicted for air core coils from Fig. 1, where the horizontal and vertical scales are normalized to $\omega$ (as is the amplitude scale in Fig. 3). Figure 1 illustrates another interesting feature of the effect of probe geometry on liftoff signal characteristics. Next to the I and Q axes, two liftoff trajectories are shown (a long-dashed line and a short-dashed line). The second case (schematic only) illustrates a type of behavior observed for certain coil geometries (Dodd, 1983). All of these flaw and liftoff responses may be predicted theoretically from Eq. (1), if the tangential field distribution is known in the XY plane. For air core coils with a

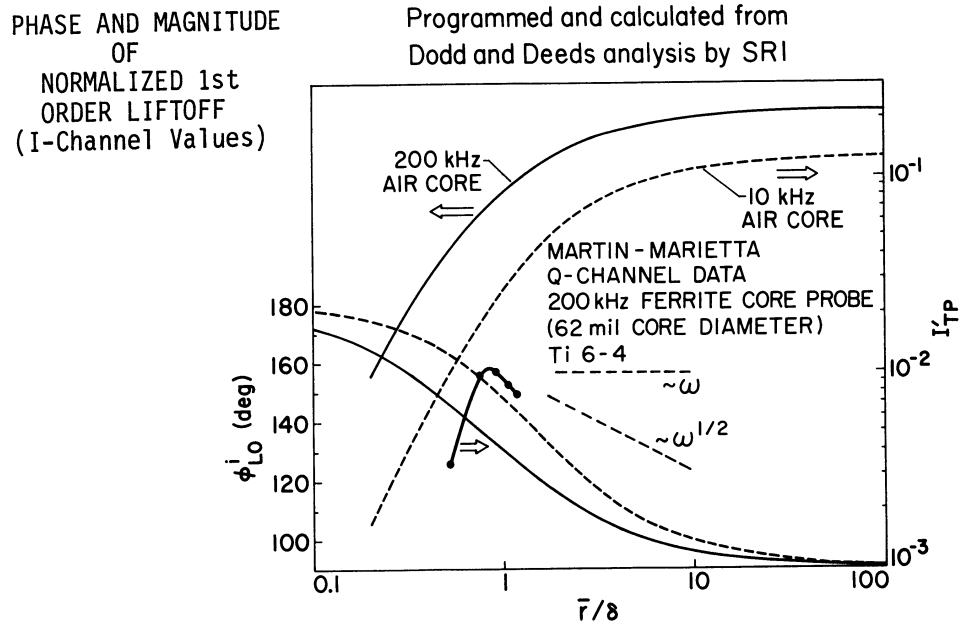


Fig. 3. Influence of probe geometry on liftoff signals.

vertical axes this can be obtained theoretically from Dodd and Deeds theory (Dodd and Deeds, 1968), and a similar calculation is possible for horizontally-oriented coils. In ferrite probes the methods of Ida (1984) or the Sabbaghs (1984) are required.

## PROBE FIELD MEASUREMENTS

Figure 4 illustrates the types of direct and perturbation field distribution measurements to be discussed here. On the left is shown

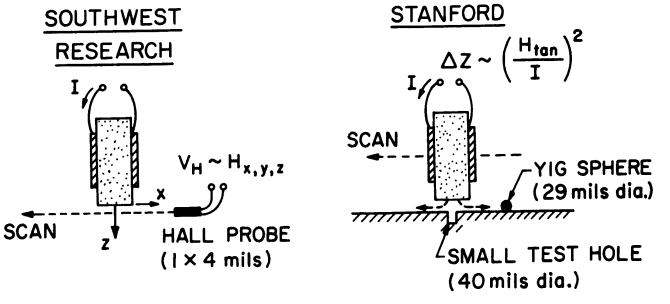


Fig. 4. Probe field measurement methods.

the Hall probe measurements performed at Southwest Research Institute (Beissner, et al., 1980) and on the right is shown the perturbation method used at Stanford. The first has the advantage of measuring the field absolutely but is difficult to perform at higher excitation frequencies, because of inductive pickup in the voltage leads [Fig. 5(a)]. It is not possible to make measurements on a probe close spaced over a workpiece, because of the probe dimensions (0.001" × 0.004") and scanning problems [Fig. 5(b)]. The second method is well adapted to measurements over a workpiece and gives directly the quantity desired in Eq. (1). However, the proportionality factor in Fig. 4 is determined by the geometry of the perturbing object (a hole 0.040" diameter by 0.25" deep in 6060 aluminum for the measurements reported here) and cannot always be calculated theoretically. The measurement must usually be calibrated from a reference. There is no restriction as to frequency, but spatial resolution is not as good as that achievable with a Hall probe. Figure 6 shows Hall probe plots along the radial direction for the air core coil of Fig. 2(b), measured at 1 kHz in air. Repeat measurements at 100 Hz gave identical results. A characteristic feature is the smoothing out of the field distribution at larger liftoff [Figs. 6(a) and 6(b)]. This effect was also observed in the ferrite core coil of Fig. 2(c), where the axial field distribution had pronounced "rabbit's ears" at small liftoff (due to the field concentration at the sharp corners of the core) but a smooth gaussian-like shape at larger liftoff. The radial field distribution [Fig. 6(c)] shows the characteristic zero on the axis. A similar radial field plot was obtained for the ferrite core probe but only at 100 mil liftoff, because of the size of the probe. Figure 7 shows measurements of the relative magnitude and phase of the squared radial field for the ferrite core probe of Fig. 2(c) over aluminum.

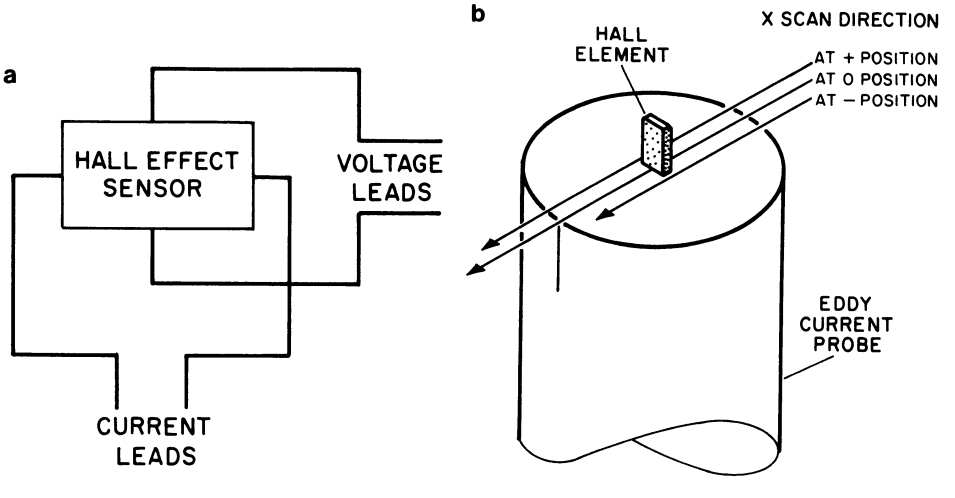


Fig. 5. Hall probe measurements. (a) Circuit connections; (b) configuration for radial field measurement.

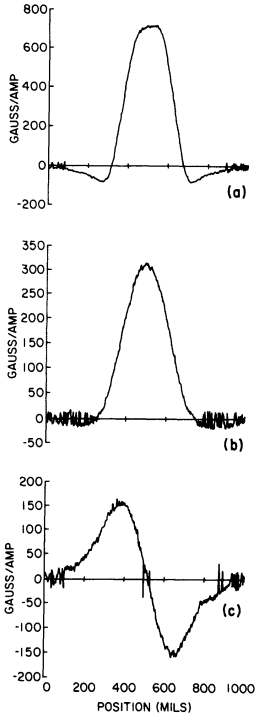


Fig. 6. Hall probe field measurements for the 10 kHz air core coil [Fig. 2(b)], scanned along a probe diameter, in air. Frequency = 1 kHz. (a) Axial field as a function of X in the 0 position of Fig. 6, liftoff = 25 mils; (b) axial field distribution, liftoff = 100 mils; (c) radial field distribution, liftoff = 100 mils.

The measurement was made at 10 kHz with the probe wear plate resting on the aluminum surfaces, therefore at much smaller liftoff than the measurements of Fig. 6.

## FIELD TRANSFORMATIONS

The change of measured probe field distribution with liftoff distance in Fig. 6 can be explained by the transformation properties of the field from one measurement plane to another. This is briefly outlined in Fig. 8. Analysis of the field distribution of an eddy current probe may be performed by using a vector potential formulation (Dodd and Deeds, 1968) or a direct field formulation (Auld and Riaziat, 1983). The second method is described here. In either case a spatial Fourier transform (or Fourier-Bessel transform for probes of circular symmetry) is performed with respect to the spatial

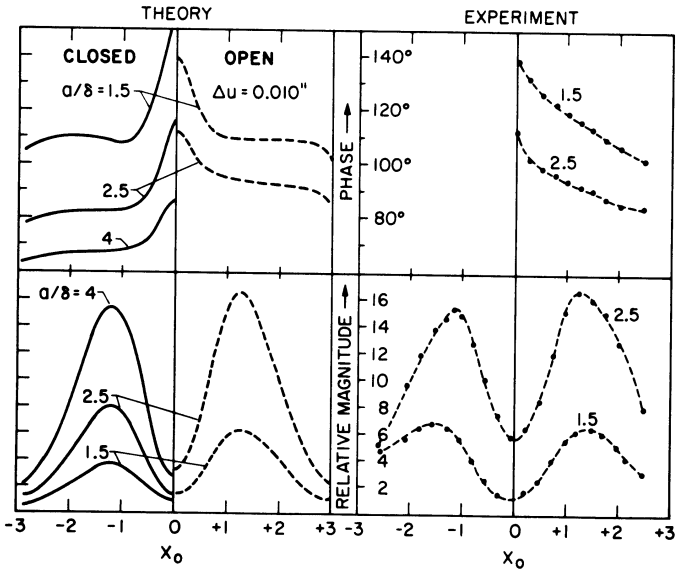


Fig. 7. ΔZ measurement of the magnitude and phase of $(H_r)^2$ over aluminum 6060 alloy for the ferrite core probe [Fig. 2(c)] measured at 10 kHz.

IN AIR

$$\vec{H}^I_{tan} = \iint \left[\vec{h}^I_{tan}(k_x,k_y)\, e^{-i\kappa Z}\right] e^{i(k_x X + k_y Y)}\, dk_x\, dk_y$$

$$\kappa = (\omega^2\mu_0\epsilon_0 - k_x^2 - k_y^2)^{1/2}$$

$$\vec{E}^I_{tan} = \frac{\omega\mu_0}{\kappa}\,\hat{Z} \times \vec{H}^I_{tan}$$

OVER METAL

$$\vec{h}^I_{tan}\, e^{-i\kappa Z} \Longrightarrow \vec{h}^I_{tan}\left(e^{-i\kappa Z} + \Gamma e^{+i\kappa Z}\right)$$

$\Gamma(k_x, k_y)$ = FUNCTION OF $\omega$, METAL CONDUCTIVITY, AND LIFTOFF

Fig. 8. Transformation of tangential magnetic field from one observation plane to another.

coordinates XY of the workpiece plane. The transform representation of the tangential magnetic field of Eq. (1) appears in this format in the first line of Fig. 8, for the case of a probe in air. Transformation of the field from one plane to another (along Z ) is governed by the exponential within the square bracket, with the exponent defined in the second line of the figure. The corresponding

tangential electric field is given in the third line. When the probe is placed over the workpiece, electromagnetic boundary conditions determined by its material properties are imposed. These are treated by adding a reflected field to the field of the probe in air (i.e., the incident field) using reflection coefficients that are easily calculated separately for each Fourier component, as stated at the bottom of the figure. It is assumed in both approaches that the presence of the metal does not affect the current distribution in the probe coil. An important feature of these calculations, in either the vector potential or the direct field approach, is that the quantity $K$ in the figure is pure imaginary over all but an extremely small part of the Fourier spectrum. For this reason the $Z$ exponential in the first line describes an exponential decay of the Fourier amplitudes with distance from the probe, the components with more rapid variations in the $XY$ plane having more rapid decay rates. Because of this, the field profile smooths out with increasing distance from the probe, as described above and illustrated in Fig. 6. One consequence is that the more rapidly varying Fourier components are lost in the noise when measurements are made at a distance from the probe, so that the measured field cannot be accurately transformed back to a plane close to the probe. This emphasizes the need for a measurement technique capable of measuring tangential fields very close to the probe.

Probe fields in air have a constant phase (Fig. 6), while the phase varies with position for a probe over a workpiece (Fig. 7). This feature is very important in the interpretation of EC signals and must be accurately quantified for precise flaw inversion. Figure 8 shows that once the tangential field has been measured in air (close to the probe itself) the field over a workpiece can always be calculated. Consequently, Hall probe field measurements in air are sufficient for completely characterizing the behavior of any air core probe (radially symmetric or not), provided they can be made sufficiently close to the probe itself. Fast Fourier transform software now exists for transforming the measured fields to any liftoff over an arbitrary workpiece (Riaziat and Auld, 1984). For ferrite core probes, in which the core properties are frequency dependent, the frequency limitations of the Hall probe may prevent measurement of a probe at its design frequency and thereby give an inaccurate calibration.

## CONCLUSION

This paper has reviewed the status of theoretical and experimental methods for characterizing the interrogating field distribution of an EC probe, a factor of the greatest importance in realizing the goal of precise reproducible quantitative NDE. Work reported here has been performed only on absolute probes but can be extended to other geometries. An extensive theoretical base exists for air

core probes. This has been widely applied only for circularly symmetric geometries but can be extended to the more general case. Numerical methods, or simple dipole modeling, are techniques available for ferrite core probes. Here, however, direct experimental measurements may be more satisfactory because of uncertain knowledge of the ferrite properties. In any case direct measurements of the probe field is an essential step in comparing an actual probe with its design properties. For this purpose it is necessary to be able to measure the probe field in air very close to the probe.

## ACKNOWLEDGEMENT

This work was sponsored by the Center for Advanced Nondestructive Evaluation, operated by the Ames Laboratory, USDOE, for the Air Force Wright Aeronautical Laboratories/Materials Laboratory and the Defense Advanced Research Projects Agency under Contract No. W-7405-ENG-82 with Iowa State University.

## REFERENCES

Auld, B. A., and Riaziat, M., 1983, Spatial frequency analysis and matched filtering in electromagnetic nondestructive evaluation, J. Appl. Phys., 54:3509.

Beissner, R. E., Matzkanin, G. A., and Teller, C. M., 1980, NDE applications of magnetic leakage methods, Nondestructive Testing Information Analysis Center, Publication NTIAC-80-1, Southwest Research Institute, San Antonio, Texas.

Dodd, C. V., and Deeds, W. E., 1968, Analytic solutions to eddy current problems, J. Appl. Phys., 39:2829.

Dodd, C. V., 1983, Private communication.

Ida, N., 1984, Development of a 3-D eddy current model for nondestructive testing phenomena, this volume.

Muennemann, F. G., Ayter, S., and Auld, B. A., 1984, Computation of Eddy Current signals and quantitative inversion with realistic probe models, this volume.

Riaziat, M., and Auld, B. A., 1984, Angular spectrum analysis applied to horizontal dipole probes and under cladding flaws, this volume.

Sabbagh, L. D., and Sabbagh, H. A., 1984, Inversion of eddy current data and the reconstruction of flaws using multifrequencies, this volume.

## DISCUSSION

G. Birnbaum (National Bureau of Standards): I think you said that the perturbation method was a relative method; is that correct?

B.A. Auld: It is relative to the extent that if you want to make it non-relative, you have to calibrate the perturbation on the object, and that may not be possible.

G. Birnbaum: Could you explain what that means, because I think I understand the perturbation theory and there's nothing relative about the theory itself. If you measure the change of impedance with or without the sample, you should, provided the perturbation is small enough, have enough indication of the field in the region that the sample occupied?

B.A. Auld: Well, I think the point, George, is this. It is true that the characteristic function is not relative, but I would hesitate to say that we know the characteristic function for a hole in a piece of metal. I don't know it. But if one could find that out, then it would be absolute, but I'm supposing when I make that remark that this is too complicated a method.

G. Birnbaum: Perhaps I was thinking of a different configuration, the same geometry you had but without the hole method, where you just rolled the sphere by and probed the field.

B.A. Auld: Yes, the sphere in the air is an absolute, yes, that's true.

S.G. Marinov (Dresser Industries): What is the depth of penetration in your case? Is it smaller than the depth of the crack or bigger?

B.A. Auld: Compared with the hole, you mean?

S.G. Marinov: Yes. Depth of penetration, what frequency do you use?

B.A. Auld: We were working with aluminum at about 10 kilohertz and the hole was about a millimeter deep and on 10 kilohertz is about--I would say the penetration depth was about comparable to the hole.

S.G. Marinov: You mean the depth of penetration is bigger than the depth of the crack; is that correct?

B.A. Auld: Well, we are not looking at cracks yet.

S.G. Marinov: Well, you consider the defect flaw.

B.A. Auld: What we considered are both cases where the crack is much deeper than the penetration depth and where the crack is much smaller than the penetration depth. As I will say presently, or

review presently, the theory is really non-existent at the present time for the case where the depths are comparable.

S.G. Marinov: I asked because in the case where the depth of penetration is bigger, you cannot consider the only single source of noise as the lift-off. You also need surface noise to ground the signal which--you understand?

B.A. Auld: If I understand you, you mean that if you are looking at lift-off noise in the presence of a flaw where the flaw is bigger than the penetration depth, that this distorts the noise distribution?

S.G. Marinov: Yes.

B.A. Auld: Okay. We haven't considered that. We have considered, or Al is going to discuss considering, the variation of lift-off noise with lift-off in the absence of a flaw, but I think it is correct that we have not considered interactions of the flaw and the lift-off. But I can well believe that's true.